THE STOCHASTIC MODELING OF A RANDOM LAMINAR WAKE PAST A CIRCULAR CYLINDER

Daniele Venturi[†] and Sandro Salvigni[†]

[†]DIENCA, Dipartimento di Ingegneria Energetica, Nucleare e del Controllo Ambientale,
Università degli Studi di Bologna

ABSTRACT

We study the random laminar wake past a circular cylinder corresponding to a random Reynolds number. The random flow is computed using two different stochastic methods, i.e. the generalized polynomial chaos and the multi-element generalized polynomial chaos method. Rigorous convergence to the correct statistics of the velocity field is established. The random flow is subsequently decomposed into random modes according to a new type of orthogonal decomposition developed in this paper. This orthogonal decomposition which is substantially built upon the proper orthogonal decomposition framework defines an optimal set of random projectors for the stochastic Navier-Stokes equations which, after a suitable averaging operation, leads to a *deterministic* temporal evolution, i.e. a system of ordinary deterministic differential equations. This allow to construct a reduced order Galerkin model of the random flow as superimposition of deterministic temporal evolution of random spatial structures. Numerical applications are presented and discussed.

1 Introduction

The proper orthogonal decomposition (POD) has been proposed by Lumley [1] for detection of spatial coherent patterns in turbulent flows. He introduced it in the field of hydrodynamics when there was a need for a mathematical definition of coherent structures in turbulence. To analyze such temporally and spatially evolving flows Aubry *et al.* [2] introduced the concept of biorthogonal decomposition which is a deterministic space-time version of the POD ([2]). One of the most remarkable feature of such a decomposition is that it gives access to the complexity of the spatial and temporal dynamics simultaneously. The flow field is decomposed into a hierarchical set of spatial and temporal orthogonal modes which are coupled. This generalizes the notion of spatial and temporal structures which, for example, can be followed through the various instabilities that the flow undergoes as Reynolds number increases. Low dimensional linear Galerkin [3; 4], non-linear Galerkin [4] and spectral viscosity models of various flows have been successfully developed by using the POD modes. Moreover, the method is a way to analyze and reconstruct [5] space time information such as numerical data and experimental data measured simultaneously at various locations by means of recently developed experimental techniques such as digital particle image velocimetry (DPIV), digital particle image thermometry (DPIT) [4], laser scanning techniques, cross-stream rakes of X-wires or magnetic resonance imaging (MRI).

It is common practice to perform the POD following the method of snapshots introduced by Sirovich [6]. However what it is neglected most of the time is that the snapshots taken form "real world" measurements and computations have random components which affect the POD decomposition significantly. Therefore there is the need to develop a theory to take into account the fact that the spectral properties of a random autocovariance are random variables and random processes.

The *quantification* of the relation between the stochastic flow and its random space-time structures extracted by the POD method is a challenging task as it involves random perturbations of the autocorrelation operator's spectral properties. Many attempts to quantify directly the statistics for noisy correlation (or covariance) matrices have been recently made by several Authors. Everson & Roberts *et al.* [9] use a Bayesian inference method to obtain posterior densities for each random eigenvalue; Sengupta & Mitra [7] propose a diagrammatic expansion and saddle point integration methods to quantify the empirical eigenvalue density; Hachem *et al.* [8] and Dozier & Silverstein [10] give a characterization of the eigenvalue density in terms of its Stieltjes transform; Hoyle & Rattray[11] use a statistical mechanics approach (variational mean-field theory) to give an analytical approximation to the eigenvalue spectral density.

An alternative approach was developed by Venturi in [12] and it based upon the Kato's perturbation theory for linear operators [13]. The statistics for the perturbed energy levels and the perturbed temporal modes are expressed in form of an explicit power series in the random flow standard deviation.

However the issue of *stochastic* low dimensional modeling and simulation is still an open question. In this paper we investigate how randomness propagates in Galerkin models of random flows. To this end we define a suitable orthogonal set of random projectors for the Navier Stokes equations. This new method lies within the possibility to obtain a representation of a random flow in terms of random weakly orthogonal spatial modes and deterministic temporal modes. The key idea is to compute a generalized polynomial chaos expansion ([15]) for the spatial modes, when given a chaos expansion for the random flow. This orthogonal decomposition defines an "optimal" set of random projectors for the stochastic Navier Stokes equations which, after a suitable averaging operation, leads to a *deterministic* temporal evolution, i.e. a system of ordinary deterministic differential equations. This allow to construct a reduced order model of the random flow as superimposition of deterministic temporal evolution of random spatial structures.

2 Decomposition of the random flow into random modes

We consider a second order random field[1] $\mathbf{u}(\mathbf{x},t;\xi)$ represented in terms of an orthogonal polynomial chaos basis $\{\Gamma_j(\xi)\}$

$$\mathbf{u}(\mathbf{x},t;\xi) = \sum_{j=0}^{\infty} \widehat{\mathbf{u}}_j(\mathbf{x},t)\,\Gamma_j(\xi)\,. \tag{1}$$

We look for a biorthogonal representation of $\mathbf{u}(\mathbf{x},t;\xi)$ in the form

$$\mathbf{u}(\mathbf{x},t;\xi) = \sum_{i=1}^{\infty} \sqrt{\mu_i}\psi_i(t)\,\mathbf{\Phi}_i(\mathbf{x};\xi)\,. \tag{2}$$

We assume that the temporal modes modes ψ_i are *strongly* orthogonal in time while the spatial modes $\mathbf{\Phi}_i$ are *weakly* orthogonal in space with respect to appropriate inner products. We denote by $(\,,)_T$ the inner product in temporal domain and by $\{\,,\}_h$ ($h=1,2,..$) different types of inner products in spatial domain. Orthogonality requirements are

$$(\psi_i,\psi_j)_T = \delta_{ij} \tag{3}$$
$$\{\mathbf{\Phi}_i,\mathbf{\Phi}_j\}_h = \delta_{ij} \quad h=1,2,3\ldots. \tag{4}$$

In this paper we consider

$$(\psi_i,\psi_j)_T := \int_T \psi_i(t)\,\psi_j(t)\,dt \tag{5}$$

and the following three types of spatial inner products

$$\{\mathbf{\Phi}_i,\mathbf{\Phi}_j\}_0 := \int_\Omega \langle\mathbf{\Phi}_i\rangle\cdot\langle\mathbf{\Phi}_j\rangle d\mathbf{x} \tag{6}$$
$$\{\mathbf{\Phi}_i,\mathbf{\Phi}_j\}_1 := \int_\Omega \langle\mathbf{\Phi}_i\cdot\mathbf{\Phi}_j\rangle d\mathbf{x} \tag{7}$$
$$\{\mathbf{\Phi}_i,\mathbf{\Phi}_j\}_2 := \int_\Omega \left(\langle\mathbf{\Phi}_i\cdot\mathbf{\Phi}_j\rangle - \langle\mathbf{\Phi}_i\rangle\cdot\langle\mathbf{\Phi}_j\rangle\right) d\mathbf{x} \tag{8}$$

where the averaging operation $\langle\cdot\rangle$ is defined as

$$\langle f\rangle = \int f(\xi)\,W(\xi)\,d\xi \tag{9}$$

and $W(\xi)$ is the joint probability density of ξ. We consider the positive definite functional

$$\|\mathbf{u}\|_h^2 := \int_T \{\mathbf{u},\mathbf{u}\}_h\,dt\,, \qquad h=0,1,2\,. \tag{10}$$

By elementary arguments of the calculus of variations we can minimize the "distance" (in the generic norm $\|\cdot\|_h$, $h=0,1,2$) between the expansion (2) and the random field $\mathbf{u}(\mathbf{x},t,\xi)$. Physically this corresponds to look for expansions which minimize the error in the mean (case $h=0$), in the second order moment (case $h=1$) and in the standard deviation (case $h=2$). It is immediate to see that

$$\|\mathbf{u}\|_1^2 = \|\mathbf{u}\|_2^2 + \|\mathbf{u}\|_0^2 \tag{11}$$

and therefore we expect that the expansion obtained form $\|\cdot\|_1$ is a sort of compromise between the optimality in the mean and in the standard deviation. It is also possible to consider other types of norms, eventually defined as suitable *functionals* of the random field being decomposed.

We minimize the error functional

$$\mathcal{E}_h[\psi_i] := \left\|\mathbf{u}(\mathbf{x},t;\xi) - \sum_{i=1}^{M}\sqrt{\mu_i}\psi_i(t)\,\mathbf{\Phi}_i(\mathbf{x},\xi)\right\|_h^2$$

with respect to an arbitrary variation of ψ_k to obtain

$$\delta_\psi\mathcal{E}_h = 0 \quad\Rightarrow\quad \psi_k(t) = \frac{1}{\sqrt{\mu_k}}\{\mathbf{u},\mathbf{\Phi}_k\}_h\,. \tag{12}$$

From (2) and the orthogonality requirements (3), (4) we always have

$$\mathbf{\Phi}_k(\mathbf{x};\xi) = \frac{1}{\sqrt{\mu_k}}\int_T \mathbf{u}(\mathbf{x},t;\xi)\,\psi_k(t)\,dt\,. \tag{13}$$

Substitution of (13) into (12) gives the temporal eigenvalue problem

$$\mu_k\psi_k(t) = \int_T \mathcal{T}_h(t,t')\,\psi_k(t')\,dt' \tag{14}$$

where

$$\mathcal{T}_h(t,t') := \{\mathbf{u}(\mathbf{x},t;\xi),\mathbf{u}(\mathbf{x},t';\xi)\}_h\,. \tag{15}$$

Depending on the choice of the inner product $\{,\}_h$ we have the following covariance kernels

$$\mathcal{T}_0(t,t') = \int_\Omega \langle\mathbf{u}(\mathbf{x},t;\xi)\rangle\cdot\langle\mathbf{u}(\mathbf{x},t';\xi)\rangle d\mathbf{x}\,, \tag{16}$$
$$\mathcal{T}_1(t,t') = \int_\Omega \langle\mathbf{u}(\mathbf{x},t;\xi)\cdot\mathbf{u}(\mathbf{x},t';\xi)\rangle d\mathbf{x}\,. \tag{17}$$

3 Chaos expansion representations

We assume that we have available a chaos expansion up to order P for the random field $\mathbf{u}(\mathbf{x},t;\xi)$ i.e.

$$\mathbf{u}(\mathbf{x},t;\xi) = \sum_{l=0}^{P}\widehat{\mathbf{u}}_l(\mathbf{x},t)\,\Gamma_l(\xi)\,. \tag{18}$$

The covariance $\mathcal{T}_h(t,t')$ has the following representation

$$\mathcal{T}_h(t,t') = \sum_{l=0}^{P}\langle\Gamma_l^2\rangle\{\widehat{\mathbf{u}}_l(\mathbf{x},t),\widehat{\mathbf{u}}_l(\mathbf{x},t')\}_h\,. \tag{19}$$

[1] This means a random field with *finite* variance. Moreover $\mathbf{x}$ denotes space, t time, ξ a set of random variables.

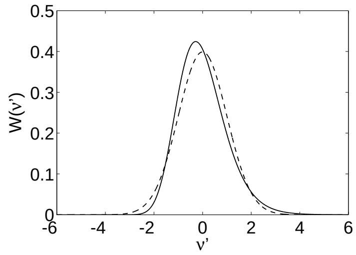

Figure 1. Probability density of ν' (—): comparison with standardized Gaussian density (− −). The polynomial chaos basis is orthogonal with respect to the probability density of ν'.

We can solve the eigenvalue problem (14) to get the eigenvalues μ_k and the temporal modes ψ_k. and subsequently compute explicitly a chaos expansion for the spatial modes as follows

$$\mathbf{\Phi}_k(\mathbf{x};\xi) = \sum_{l=0}^{P} \widehat{\mathbf{\Phi}}_{kl}(\mathbf{x})\Gamma_l(\xi)\,. \tag{20}$$

where

$$\widehat{\mathbf{\Phi}}_{kj}(\mathbf{x}) = \frac{1}{\sqrt{\mu_k}}\int_T \widehat{\mathbf{u}}_j(\mathbf{x},t)\,\psi_k(t)\,dt\,. \tag{21}$$

4 Application to random laminar wake past a cylinder

In this section we study to the random laminar wake past a circular cylinder corresponding to a random Reynolds number. First we simulate the random flow using the generalized polynomial chaos [14; 15] and the multi-element generalized polynomial chaos [16] method so that we can and establish rigorous convergence to the correct statistics. Subsequently we decompose the flow according to the new type of expansion we have introduced in §2 and we study the low dimensional model arising form random projection.

In order to construct the generalized chaos basis we need an analytical expression for the probability density of $\nu = 1/Re$ (random input). We assume that the Reynolds number Re is Gaussian distributed, conditioned to $Re > 0$, with mean μ and standard deviation σ. It is useful to perform the following decomposition

$$\nu = \nu_0 + \sigma_\nu \nu' \tag{22}$$

where $\nu' = (\nu - \nu_0)/\sigma_\nu$ is a random variable with zero mean, standard deviation 1 and probability density given by

$$W(\nu') = \frac{\sigma_\nu e^{-\frac{\left(\mu - \frac{1}{(\sigma_\nu y+\nu_0)}\right)^2}{2\sigma^2}}}{\left[\int_0^\infty \frac{1}{\sqrt{2\pi}\sigma} e^{-\frac{(\mu-t)^2}{2\sigma^2}}dt\right](\sigma_\nu y+\nu_0)^2\sqrt{2\pi}\sigma}\,. \tag{23}$$

This function is drawn in figure 1 for $\mu = 100$ and $\sigma = 10$ together with the normal distribution. The generalized chaos expansion for the random flow corresponding to a Gaussian Reynolds number is constructed according to the measure (23).

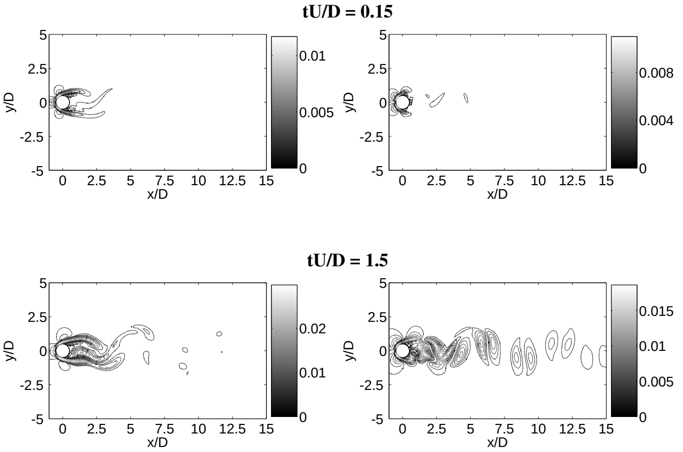

Figure 2. Standard deviations of velocity components at different time instants. Streamwise component (left); crossflow component (right).

4.1 Polynomial chaos representation of Navier-Stokes equations with random Reynolds number

We consider the expansion

$$\mathbf{v}(\mathbf{x},t;\xi) = \sum_{j=0}^{P} \widehat{\mathbf{v}}_j(\mathbf{x},t)\Gamma_j(\xi) \tag{24}$$

where generalized chaos basis $\{\Gamma_j\}$ is orthogonal with respect to the measure (23). Substitution of (24) into the Navier-Stokes equation and subsequent projection onto $\{\Gamma_j\}$ leads to the following system of partial differential equations ($k = 0,..,P$)

$$\frac{\partial \widehat{\mathbf{v}}_k}{\partial t} + \sum_{i,j=0}^{P} \frac{e_{ijk}}{e_{0kk}}(\widehat{\mathbf{v}}_i\cdot\nabla)\widehat{\mathbf{v}}_j = \nabla\widehat{p}_k + \nu_0\nabla^2\widehat{\mathbf{v}}_k + \sigma_\nu \sum_{j=0}^{P}\frac{e_{1jk}}{e_{0kk}}\nabla^2\widehat{\mathbf{v}}_j \tag{25}$$

$$\nabla\cdot\widehat{\mathbf{v}}_k = 0 \tag{26}$$

where

$$e_{ijk} = \int \Gamma_i(\nu')\Gamma_j(\nu')\Gamma_k(\nu')W(\nu')d\nu'\,. \tag{27}$$

As initial condition for this system we use a fully converged deterministic wake at $Re = 100$. In figure 2 we show how the uncertainty due to the random Reynolds number propagates in the wake at different time instants. In figure 3 we show a comparison between the generalized polynomial chaos and the multi-element method [16]. As expected, since the period of integration is quite small ($TU/D = 6$) the generalized polynomial chaos simulation and and the multi-element simulation give the same results.

4.2 Stochastic eigen-decomposition and mode analysis

We have extracted 41 equispaced snapshots of the random flow field, including the first one which is deterministic, in one shedding period of the mean flow. We decompose the random velocity field $\mathbf{v}(\mathbf{x},t;\xi)$ into a mean flow with a superimposed

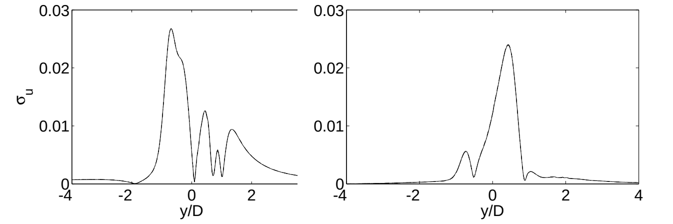

Figure 3. Convergence of ME-gPC method. Standard deviations of velocity components along the crossline $x/D = 2$ at time $tU/D = 3.75$. Streamwise component (a); crossflow component (b). gPC (—)(order 3), ME-gPC ($\cdots$) (2 elements, order 3), ME-gPC ($- \cdot -$) (4 elements, order 3), ME-gPC ($- -$) (10 elements, order 3).

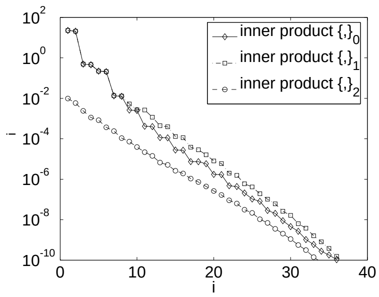

Figure 4. Eigenvalues of the covariances (19) computed using different inner products.

random fluctuation[2]

$$\mathbf{v}(\mathbf{x},t;\xi) = \mathbf{U}(\mathbf{x}) + \mathbf{u}(\mathbf{x},t;\xi)\,, \tag{28}$$

where

$$\mathbf{U}(\mathbf{x}) = \frac{1}{|T|}\int_T \langle \mathbf{v}(\mathbf{x},t;\xi)\rangle\, dt = \frac{1}{|T|}\int_T \mathbf{v}_0(\mathbf{x},t)\, dt\,. \tag{29}$$

We expand $\mathbf{u}$ into our generalized POD series

$$u^k(\mathbf{x},t;\xi) = \sum_{j=0}^{M} \psi_j(t)\,\Phi_j^k(\mathbf{x};\xi)\,, \quad k = 1,..,d\,. \tag{30}$$

The random POD basis $\{\mathbf{\Phi}_k(\mathbf{x};\xi)\}$ is *strongly* divergence free since

$$\nabla\cdot\mathbf{\Phi}_k(\mathbf{x};\xi) = \frac{1}{\sqrt{\mu_k}}\int_T \nabla\cdot\mathbf{u}(\mathbf{x},t;\xi)\,\psi_k(t)\, dt = 0\,. \tag{31}$$

The eigenvalues of the covariances (19) are shown in figure 4. Figure 5 shows the streamwise component of the mean and the standard deviation of the normalized spatial modes obtained using the inner product $\{,\}_1$.

4.3 Low dimensionality of the random wake

We study convergence of the mean and the standard deviation of the flow as function of the dimensionality of the expansion M.

[2]There are 2 ways to define the "mean" flow here. One is a deterministic mean $\mathbf{U}(\mathbf{x}) = \frac{1}{|T|}\int_t \langle \mathbf{v}(\mathbf{x},t;\xi)\rangle dt$. The other one is a stochastic time average $\mathbf{U}(\mathbf{x};\xi) = \frac{1}{|T|}\int_t \mathbf{v}(\mathbf{x},t;\xi)\, dt$. We use the deterministic mean.

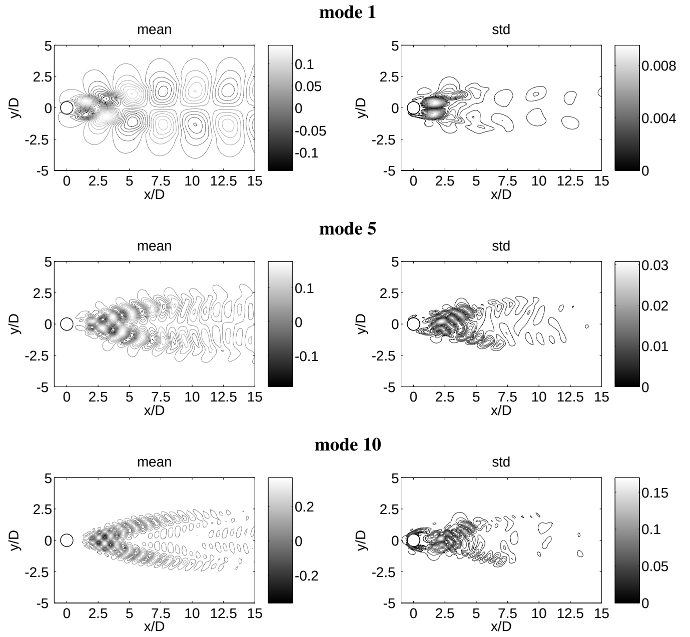

Figure 5. Streamwise component of normalized random spatial modes obtained using the second order moment inner product $\{,\}_1$: mean (left) and standard deviation (right).

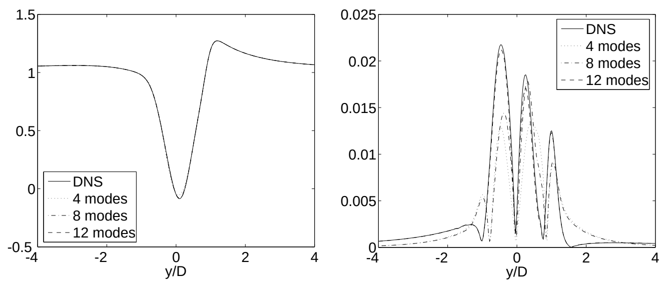

Figure 6. Mean (left) and standard deviation (right) of streamwise velocity component along the crossline $x/D = 2$ as function of the number of modes: convergence to stochastic DNS simulation. The orthogonal expansion is obtained in the second order moment inner product $\{,\}_1$.

We have the expressions

$$\langle \mathbf{u}^{(M)}\rangle = \sum_{k=1}^{M} \sqrt{\mu_k}\,\psi_k \widehat{\mathbf{\Phi}}_{k0}\,, \tag{32}$$

$$\sigma_{\mathbf{u}^{(M)}} = \left(\sum_{l=1}^{P}\left(\sum_{k=1}^{M}\sqrt{\mu_k}\,\psi_k\widehat{\mathbf{\Phi}}_{kl}\right)^2 \langle \Gamma_l^2\rangle\right)^{\frac{1}{2}}\,. \tag{33}$$

Figure 6 shows convergence of the mean and the standard deviation of the streamwise velocity component as function of the the number of POD modes. The orthogonal expansion is obtained in the second order moment inner product $\{,\}_1$.

We define the global error in the $L_2(\Omega\times T)$ norm as follows

$$\varepsilon_{\langle \mathbf{u}\rangle} = \left\|\langle \mathbf{u}\rangle - \langle \mathbf{u}^{(M)}\rangle\right\|_{\Omega\times T} \tag{34}$$

$$\varepsilon_{\sigma_{\mathbf{u}}} = \left\|\sigma_{\mathbf{u}} - \sigma_{\mathbf{u}^{(M)}}\right\|_{\Omega\times T} \tag{35}$$

where

$$\|\mathbf{g}\|^2_{\Omega\times T} := \int_T\int_\Omega \mathbf{g}\cdot\mathbf{g}\, d\mathbf{x}\, dt\,. \tag{36}$$

In figure 7 we show the errors (34) and (35) with respect to

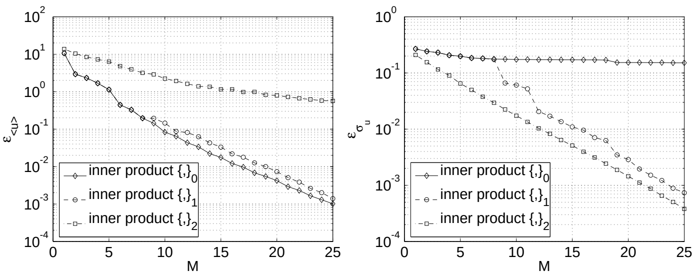

Figure 7. Error in the L^2 norm with respect to DNS of POD projection versus the number of modes. Error in the mean (left) and in the standard deviation (right). Shown are results obtained using different inner products.

DNS versus the number of modes using different types of inner products. As previously discussed we see that the expansion obtained using the inner product $\{,\}_1$ is a sort of compromise between $\{,\}_2$ and $\{,\}_0$ for what concerns the error in the mean and in the standard deviation. Also we note that the error plots for the cases $h = 0$ and $h = 2$ represent the *minimum errors achievable on the mean and the standard deviation* respectively for a certain number of POD modes.

5 Random projection of Navier-Stokes equations

The deterministic nature of the temporal modes opens the possibility to build up a *stochastic* low dimensional model of the random flow. In fact the weak orthogonality of random spatial modes can be used to define random POD projectors in a quite straightforward way. To this end we consider the Navier-Stokes equations (double index here means summation)

$$\frac{\partial v^k}{\partial t} + v^j \frac{\partial v^k}{\partial x^j} = -\frac{\partial p}{\partial x^k} + \nu \frac{\partial^2 v^k}{\partial x^j \partial x^j} \tag{37}$$

Substitution of (28) into (37) yields

$$\frac{\partial u^k}{\partial t} + U^j \frac{\partial U^k}{\partial x^j} + U^j \frac{\partial u^k}{\partial x^j} + u^j \frac{\partial U^k}{\partial x^j} + u^j \frac{\partial u^k}{\partial x^j} = -\frac{\partial p}{\partial x^k} + \nu \frac{\partial^2 u^k}{\partial x^j \partial x^j} + \nu \frac{\partial^2 U^k}{\partial x^j \partial x^j}\,. \tag{38}$$

We expand $\mathbf{u}$ in a generalized POD series (30) and we perform a Galerkin projection of Navier Stokes equations onto the (*not* normalized) random, divergence free, spatial modes $\mathbf{\Phi}_j$ using the generic inner product $\{,\}_h$. We obtain

$$\{\Phi_l^k \frac{\partial \psi_l}{\partial t} + U^j \frac{\partial U^k}{\partial x^j} + U^j \psi_l \frac{\partial \Phi_l^k}{\partial x^j} + \psi_l \Phi_l^j \frac{\partial U^k}{\partial x^j} + \psi_l \Phi_l^j \psi_n \frac{\partial \Phi_n^k}{\partial x^j} - \nu \left(\frac{\partial^2 U^k}{\partial x^j \partial x^j} + \psi_l \frac{\partial^2 \Phi_l^k}{\partial x^j \partial x^j} \right), \Phi_m^k\}_h = 0 \ . \tag{39}$$

The pressure term drops out because of the divergence free constraint and the boundary conditions[3]. The following system of ordinary differential equations is obtained

$$\boxed{\frac{d\psi_m}{dt} = \frac{1}{\mu_m} \left(-\mathcal{C}_m^{(h)} - \mathcal{L}_{ml}^{(h)} \psi_l - \mathcal{Q}_{mln}^{(h)} \psi_l \psi_n \right)} \tag{41}$$

The initial condition for ψ_m is

$$\psi_m(0) = \frac{1}{\sqrt{\mu_m}} \{\mathbf{u}(\mathbf{x}, 0; \xi), \mathbf{\Phi}_m(\mathbf{x}; \xi)\}_h \,. \tag{42}$$

Explicit expressions for $\mathcal{C}_m^{(h)}$, $\mathcal{L}_{ml}^{(h)}$ and $\mathcal{Q}_{mln}^{(h)}$ for $h = 0, 1, 2$ will be reported elsewhere.

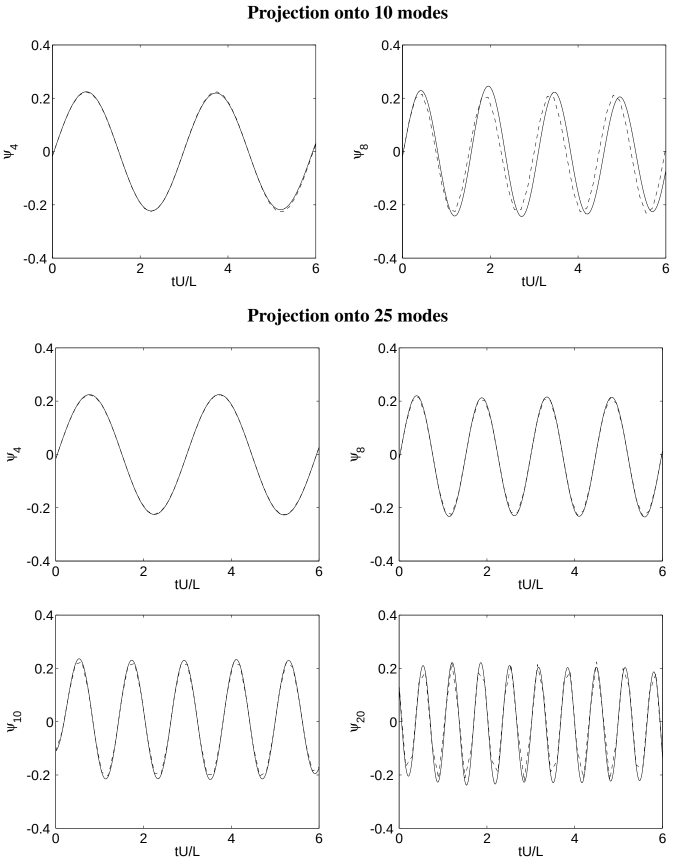

Figure 8. Case $h = 1$ (second order moment inner product). Comparison between temporal evolution predicted by the system (41) (-) and the DNS based evolution (- -)

5.1 POD simulation of the random wake

In figure 8 we compare the temporal modes extracted from the DNS to the temporal evolution predicted by the system (41). We define the time dependent error in the L_2 spatial norm for the mean and the standard deviation of the velocity as follows

$$e_{\langle \mathbf{u} \rangle}(t) = \left\| \langle \mathbf{u} \rangle - \langle \mathbf{u}^{(M)} \rangle \right\|_\Omega \tag{43}$$

$$e_{\sigma_{\mathbf{u}}}(t) = \left\| \sigma_{\mathbf{u}} - \sigma_{\mathbf{u}^{(M)}} \rangle \right\|_\Omega \tag{44}$$

[3] In fact by the Gauss formula we have

$$\int_\Omega \mathbf{\Phi}_m \cdot \nabla p d\mathbf{x} = -\int_\Omega \nabla \cdot \mathbf{\Phi}_m p d\mathbf{x} + \int_{\partial\Omega} p (\mathbf{\Phi}_m \cdot \mathbf{n}) d\mathbf{x} = 0 + \int_{\partial\Omega} p (\mathbf{\Phi}_m \cdot \mathbf{n}) d\mathbf{x}. \tag{40}$$

The last integral is 0 on all sides where we have deterministic Dirichlet B.C. ($\mathbf{\Phi}_m \equiv 0$). It is 0 on the periodic sides of the domain as they have opposite orientations in the integration path and it is zero on the outflow where $p \equiv 0$.

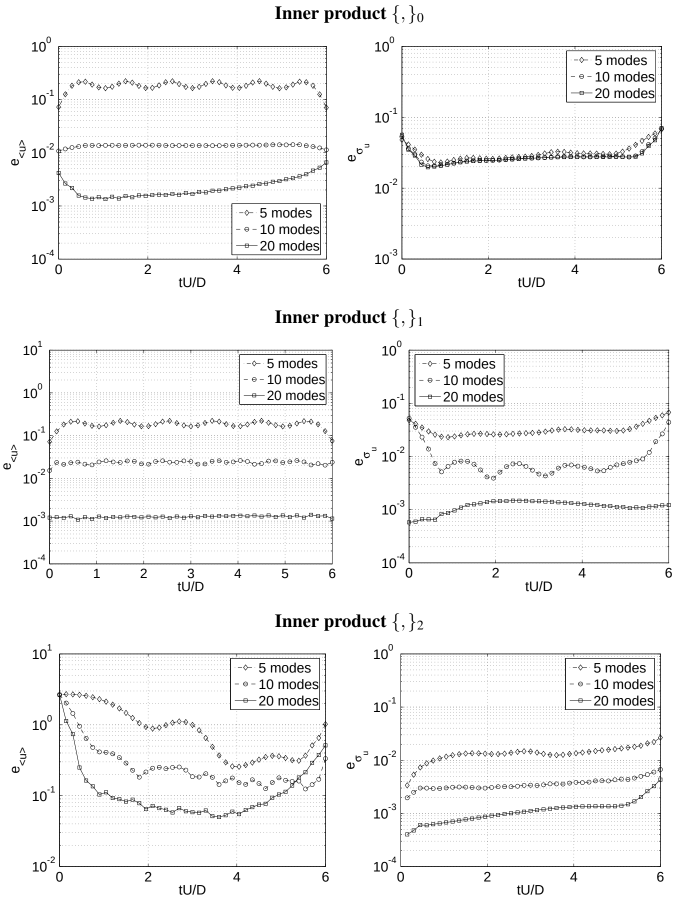

Figure 9. POD Simulation errors as function of time. Left: error in the mean (43); right: error in the standard deviation (44). Shown are results obtained using different types of inner products.

where

$$\|\mathbf{u}\|_{\Omega}^{2} = \int_{\Omega} \mathbf{u} \cdot \mathbf{u} d\mathbf{x}. \tag{45}$$

In figure 9 we show (43) and (43) as function of the number of modes for the inner product $\{,\}_1$, $\{,\}_1$ and $\{,\}_2$ respectively.

6 Summary and conclusions

We have studied the random laminar wake past a circular cylinder corresponding to a random Reynolds number. We simulated the random flow using the generalized polynomial chaos method and the multi element generalized polynomial chaos method to establish rigorous convergence to the correct statistics. Subsequently we decomposed the random flow according to a new type of expansion developed in §2 and we constructed in §5 a low dimensional stochastic model of the wake though Galerkin projection onto random spatial modes. We have found that the accuracy of this reduced order model significantly depends on the type of inner product $\{,\}_h$ used to decompose the random flow.

Subsequent research will focus on obtaining better low dimensional representations of the random flow in order to achieve optimal convergence and provide a new tool for detection of spatial coherent patterns in turbulent flows.

References

[1] Lumley J.L. *Stochastic tools in turbulence*. Academic Press, 1970.

[2] Aubry N. On the hidden beauty of the proper orthogonal decomposition. *Theoret. Comput. Fluid Dynamics*, 2:339–352, 1991.

[3] Noack B.R., Afanasiev K., Morzyński M., Tadmor G. and Thiele F. A hierarchy of low dimensional models for the transient and post-transient cylinder wake. *J. Fluid Mech.*, 497:335–363, 2003.

[4] Ma X., Karniadakis G.E., Park H. and Gharib M. DPIV-driven simulation: a new computational paradigm. *Proc. Royal Soc. A*, 459:547–565, 2003.

[5] Venturi D. and Karniadakis G.E. Gappy data and reconstruction procedures for flow past a cylinder. *J. Fluid Mech.*, 519:315–336, 2004.

[6] Sirovich L. Turbulence and the dynamics of coherent structures: 1, 2, 3. *Quart. Appl. Math.*, 45(3):561–590, 1987.

[7] Sengupta M. and Mitra P.P. Distribution of singular values of some random matrices. *Phys. Rev. E*, 60:3389–3392, 1999.

[8] Hachem W., Loubaton P. and Najim J. On the Empirical Distribution of Eigenvalues of a Gram matrix with a given variance profile. eprint arXiv:math/0411333, 2004.

[9] Everson R.M. and Roberts S.J. Inferring the eigenvalues of covariance matrices from limited, noisy data. *IEEE Trans. Sig. Proc.*, 48(7):2083–2091, 2000.

[10] Dozier R.B. and Silverstein J.W. On the Empirical Distribution of Eigenvalues of Large Dimensional Information Plus-Noise Type Matrices. *Journal of Multivariate Analysis*, 98 (4):678–694, 2004.

[11] Hoyle D.C. and Rattray M. A Statistical Mechanics Analysis of Gram Matrix Eigenvalue Spectra. In John Shawe-Taylor and Yoram Singer, editor, *Learning Theory, 17th Annual Conference on Learning Theory, COLT 2004, Banff, Canada, July 1-4, 2004, Proceedings*, pages 579–593. Springer, 2004.

[12] Venturi D. On proper orthogonal decomposition of randomly perturbed fields with applications to flow past a cylinder and natural convection over a horizontal plate. *J. Fluid Mech.*, 559:215-254, 2006.

[13] Kato T. *Perturbation theory for linear operators*. Springer-Verlag, fourth edition, 1995.

[14] Xiu D. and Karniadakis G.E. The Wiener–Askey polynomial chaos for stochastic differential equations. *SIAM J. Sci. Comput.*, 24(2):619–644, 2002.

[15] Xiu D. and Karniadakis G.E. Modeling uncertainty in flow simulations via generalized polynomial chaos. *J. Comp. Phys.*, 187:137–167, 2003.

[16] Wan X. and Karniadakis G.E. Multi-element generalized polynomial chaos for arbitrary probability measures. *SIAM J. Sci. Comput.*, 28(3):901–928, 2006.